

A Search for WIMPs with the First Five-Tower Data from CDMS

Z. Ahmed,² D.S. Akerib,³ S. Arrenberg,¹⁶ M.J. Attisha,¹ C.N. Bailey,³ L. Baudis,¹⁶ D.A. Bauer,⁴ J. Beaty,¹⁵ P.L. Brink,⁹ T. Bruch,¹⁶ R. Bunker,¹² B. Cabrera,⁹ D.O. Caldwell,¹² J. Cooley,⁹ P. Cushman,¹⁵ F. DeJongh,⁴ M.R. Dragowsky,³ L. Duong,¹⁵ J. Emes,⁵ E. Figueroa-Feliciano,⁶ J. Filippini,¹¹ M. Fritts,¹⁵ R.J. Gaitskell,¹ S.R. Golwala,² D.R. Grant,³ J. Hall,⁴ R. Hennings-Yeomans,³ S. Hertel,⁶ D. Holmgren,⁴ M.E. Huber,¹³ R. Mahapatra,¹² V. Mandic,¹⁵ K.A. McCarthy,⁶ N. Mirabolfathi,¹¹ H. Nelson,¹² L. Novak,⁹ R.W. Ogburn,⁹ M. Pyle,⁹ X. Qiu,¹⁵ E. Ramberg,⁴ W. Rau,⁷ A. Reisetter,¹⁵ T. Saab,¹⁴ B. Sadoulet,^{5,11} J. Sander,¹² R. Schmitt,⁴ R.W. Schnee,¹⁰ D.N. Seitz,¹¹ B. Serfass,¹¹ K.M. Sundqvist,¹¹ M. Tarka,¹⁶ A. Tomada,⁹ G. Wang,² S. Yellin,^{9,12} J. Yoo,⁴ and B.A. Young⁸

(CDMS Collaboration)

¹*Department of Physics, Brown University, Providence, RI 02912, USA*

²*Department of Physics, California Institute of Technology, Pasadena, CA 91125, USA*

³*Department of Physics, Case Western Reserve University, Cleveland, OH 44106, USA*

⁴*Fermi National Accelerator Laboratory, Batavia, IL 60510, USA*

⁵*Lawrence Berkeley National Laboratory, Berkeley, CA 94720, USA*

⁶*Department of Physics, Massachusetts Institute of Technology, Cambridge, MA 02139, USA*

⁷*Department of Physics, Queen's University, Kingston, Ont., Canada, K7L 3N6*

⁸*Department of Physics, Santa Clara University, Santa Clara, CA 95053, USA*

⁹*Department of Physics, Stanford University, Stanford, CA 94305, USA*

¹⁰*Department of Physics, Syracuse University, Syracuse, NY 13244*

¹¹*Department of Physics, University of California, Berkeley, CA 94720, USA*

¹²*Department of Physics, University of California, Santa Barbara, CA 93106, USA*

¹³*Departments of Phys. & Elec. Engr., University of Colorado Denver, Denver, CO 80217, USA*

¹⁴*Department of Physics, University of Florida, Gainesville, FL 32611, USA*

¹⁵*School of Physics & Astronomy, University of Minnesota, Minneapolis, MN 55455, USA*

¹⁶*Physics Institute, University of Zürich, Zürich, Switzerland*

We report first results from the Cryogenic Dark Matter Search (CDMS II) experiment running with its full complement of 30 cryogenic particle detectors at the Soudan Underground Laboratory. This report is based on the analysis of data from 15 Ge detectors (3.75 kg) acquired between October 2006 and July 2007 for an effective exposure of 121.3 kg-d (averaged over recoil energies 10–100 keV, weighted for a weakly interacting massive particle (WIMP) mass of 60 GeV/c²). A blind analysis, incorporating improved techniques for rejecting surface events and estimating background leakage into the signal region, resulted in zero observed events. This analysis sets an upper limit on the WIMP-nucleon spin-independent cross section of $6.6 \times 10^{-44} \text{ cm}^2$ ($4.6 \times 10^{-44} \text{ cm}^2$ when combined with previous CDMS data) at the 90% confidence level for a WIMP mass of 60 GeV/c². By excluding new parameter space for WIMP dark matter with masses above 42 GeV/c² this work significantly restricts some of the favored supersymmetric models.

PACS numbers: 14.80.Ly, 95.35.+d, 95.30.Cq, 95.30.-k, 85.25.Oj, 29.40.Wk

Within the current theoretical framework, cosmological observations [1] imply the existence of non-baryonic dark matter that drives structure formation on large scales and dominates galactic and extra-galactic kinematics. Weakly Interacting Massive Particles (WIMPs) [2], with a mass between a few tens of GeV/c² to a few TeV/c², form a generic class of dark matter candidates, motivated [3, 4] both by the measured value of the cosmological density and by the need to stabilize the standard model of particle physics at the weak scale.

Such WIMPs should be distributed in the halo surrounding the Milky Way and scatter in terrestrial particle detectors. Their coherent scattering on nuclei should lead to a roughly exponential energy-transfer spectrum with a mean energy between 10 and 30 keV [4, 5]. The event rate is expected to be below 0.1 event per kilogram of target

per day, much smaller than radioactivity rates in most materials. A number of technologies, most based on the recognition of nuclear recoils among the electron recoils produced by gammas and betas from radioactivity, are starting to reach this sensitivity level, corresponding to a scalar (“spin independent”) WIMP-nucleon scattering cross-section on the order of 10^{-43} cm^2 . Such “direct” searches for WIMP elastic scattering are complementary to “indirect” searches for their annihilation products in our galaxy and to the searches for supersymmetry or large additional dimensions at particle colliders [6].

The Cryogenic Dark Matter Search (CDMS II) operates a total of 19 germanium (250 g each) and 11 silicon (100 g each) solid-state detectors at 50 mK in the Soudan Underground Laboratory. Each detector is a 3 inch diameter disk, 1 cm thick [7, 8]. Athermal phonons

produced by a particle interaction are detected by four superconducting sensors covering each quadrant on one of the flat faces. Ionization is drifted by an electric field of 3 V/cm and collected on two concentric electrodes on the opposite face. The ratio of ionization pulse height to phonon recoil energy (“ionization yield”) allows us to discriminate nuclear from electron recoils with a rejection factor of $> 10^4$. Improvements made since our previous publications [9, 10] include deployment of 18 additional detectors, increased exposure, greater cryogenic stability, faster data acquisition, enhanced monitoring and control of data quality, and improved analysis techniques. We report on data from 15 Ge detectors (3.75 kg) acquired in two periods (designated as runs 123 and 124) between October 2006 and July 2007. The analysis for the remaining detectors is ongoing and a full account of the data taken in this period will be forthcoming.

Electron recoils within $\sim 10 \mu\text{m}$ of the detector surface suffer from a suppressed charge signal. The resulting reduction in ionization yield can be sufficient for a surface electron recoil to be misclassified as a nuclear recoil. Signal timing and amplitude comparisons among the four phonon sensors and between the phonon and charge signals provide effective discrimination against these events, improving our overall rejection of electron recoils to $> 10^6$. Based on this rejection power, CDMS detector technology has provided the means to perform the only direct detection experiment with less than one expected background event in the signal region.

Surface events mainly occur due to radioactive contamination on detector surfaces, or as a result of external gamma-ray interactions releasing low-energy electrons from surfaces near the detectors. A correlation analysis between alpha-decay and surface-event rates provides evidence that ^{210}Pb (a daughter-product of ^{222}Rn) is a major component of our surface event background [11]. Surface events generated *in situ* at Soudan, either from calibration with a ^{133}Ba source or naturally present in the WIMP search data, are studied to estimate the surface event leakage into the signal region for each detector.

Neutrons induced by radioactive processes or by cosmic-ray muons interacting near the apparatus can generate nuclear-recoil events that cannot be distinguished from possible dark matter interactions on an event by event basis. Passive Pb and polyethylene shielding is surrounded by an active muon veto to detect muons which could produce neutrons inside the shield, and also to detect showers accompanying cosmogenic neutrons penetrating the shield from outside.

Monte Carlo simulations of the muon primaries and subsequent neutron production and transport have been conducted with FLUKA [12], MCNPX [13] and GEANT4 [14] to predict the expected background from cosmogenic neutrons. We normalized the results to the observed veto-coincident multiple-scatter nuclear-recoil rate which led to an expected background from this source of < 0.1

events in our WIMP-search data.

Monte Carlo simulations of neutrons induced by nuclear decay were also performed. These simulations were based on gamma-ray measurements of daughter products of U and Th in the materials of our experimental setup and the assumption of secular equilibrium. The estimated background is < 0.1 event, dominated by the deduced upper limit of U in the Pb shield. Direct measurements of U in Pb [15] from the same source as the Pb used in our setup suggest a considerably lower contamination.

To avoid bias, we performed a blind analysis. An event mask was defined during initial data reduction to remove events in and near the signal region from WIMP search data sets while developing the analysis. This mask was based on primary quantities not subject to refinement during the analysis process, keeping the event selection constant throughout the analysis process. After WIMP selection criteria were finalized, the masking was relaxed to cover only the actual signal region to aid in background estimation.

Data from gamma (^{133}Ba) and neutron (^{252}Cf) sources were used to determine data selection criteria (“cuts”) that define the signal region, to monitor detector stability, and to characterize detector performance. Calibration data taken regularly with ^{133}Ba generated over 28 million electron recoil events between 10–100 keV, exceeding by a factor of thirty the number of comparable events in the low-background data. Alternating calibration events were assigned to two statistically independent samples to allow unbiased characterization of cut performance. Over 600,000 events were recorded using the ^{252}Cf source during five separate periods throughout the runs, including more than 10^5 nuclear recoils used to characterize WIMP acceptance.

Since WIMPs will not interact more than once in our apparatus, we require that a candidate dark matter event deposit energy in one and only one detector (“single scatter event”: signal $> 6\sigma$ above mean phonon noise in one detector and $< 4\sigma$ above mean phonon noise in all others). For three detectors which exhibited relatively poor phonon performance it was further required that the ionization signals not exceed their respective 4σ noise thresholds. All 30 detectors contributed to active vetoing of multiple scatter events.

In this analysis we consider only the Ge detectors for WIMP search. Of the 19 Ge detectors, three suffering reduced performance from readout failures and one from relatively poor resolution, have been left out of the present report. The remaining 15 Ge detectors were used for the run 123 analysis. Eight of these detectors were excluded from WIMP search during the shorter run 124 due to systematic variations in performance between the two runs. Along with the Si detectors, the analysis of data from these detectors is ongoing and remains blind.

Real-time monitoring of detector performance was

challenging due to the low event rate (~ 0.2 Hz) of the WIMP search data. Both calibration and WIMP search data (signal region excluded) were used to study detector stability and identify periods of poor performance. A standard set of one- and two-dimensional event parameter distributions were identified and each data series was compared to a template via Kolmogorov-Smirnov testing. Automated comparisons were generated following each data acquisition, allowing persistent problems to be identified and corrected. A new cut was also developed to identify periods of temporary poor ionization collection, during which bulk electron recoil events may leak into the signal region.

In addition to quality and topology cuts, WIMP candidates are required to satisfy a fiducial volume cut based on the partitioning of energy between the two concentric charge electrodes. Candidates must also lie within a signal region delimited by further cuts on ionization yield and phonon timing. Analyses of previous runs showed that using two phonon timing parameters - the risetime and the delay relative to the fast ionization signal - provided good rejection of surface-electron recoils while retaining reasonable acceptance of nuclear recoils. As in previous analyses we sum these two quantities to form a single timing parameter.

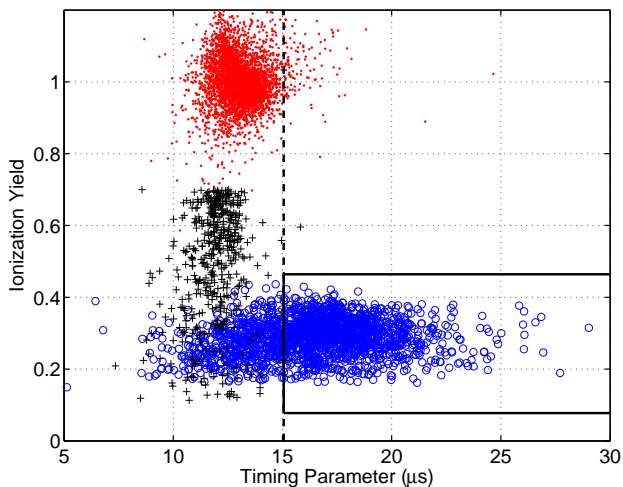


FIG. 1: Ionization yield versus timing parameter (see text) for calibration data in one of our Ge detectors, with recoil energies in the range 10–100 keV. The yield is normalized to unity for typical bulk-electron recoils (dots, light red; from ^{133}Ba gamma rays). Low-yield ^{133}Ba events (+, black), attributed to surface electron recoils, have small values of timing parameter, allowing discrimination from neutron-induced nuclear recoils from ^{252}Cf (o, medium blue), which show a wide range of timing parameter values. The vertical dashed line shows the minimum timing parameter allowed for candidate dark matter events, and the box shows the approximate signal region, which is in fact weakly energy dependent. (Color online.)

The timing and amplitudes of the phonon signals vary

slightly depending on the position and energy of each event, and we must compensate for these variations in order to maintain effective surface event rejection. We calibrate for these effects using an empirical look-up table based on our extensive electron recoil calibrations. The present analysis incorporates energy dependencies into this look-up table alongside position dependencies for the first time, enabling improved surface event discrimination.

Event reconstruction at large radius remains imperfect due to degeneracies in the phonon position quantities which inform this look-up table. In particular, since the look-up table was based only on events with no energy in the outer charge electrode, a small number of high radius events were identified with the wrong branch in the double-valued space of timing versus radius and thus miscalibrated. An additional cut on the position-related phonon quantities was developed for this analysis based on calibration data to remove events in problematic regions of the look-up table. In the future, this correction will be included directly in the event position correction by expanding the space to include events in the outer charge channel.

Figure 1 shows an example of the distribution of the timing parameter in calibration data (gammas, gamma-induced surface events and neutron-induced nuclear recoils). To effectively remove surface events, we require that candidate dark matter events exceed a minimum value for this timing parameter (“timing cut”). The timing cut is determined individually for each detector by setting an allowed maximum passage fraction in a subset of the ^{133}Ba calibration data. A consistency cut is also defined which requires that candidate dark matter events are consistent with the nuclear-recoil event distribution (less than 4σ deviation from the mean neutron distribution for the difference between delay and risetime). The performance of this cut is superior to that of earlier analyses due to improvements to the look-up table.

We estimate an expected background of 0.6 ± 0.5 events in this WIMP search exposure due to surface interactions. This estimate is obtained by multiplying the number of unvetted single-scatter events in each detector rejected only by the timing cut by the ratio of the number of unrejected multiple-scatter events inside the 2σ nuclear recoil region. Further estimation techniques are under consideration which should reduce this error bar substantially.

The acceptance of our analysis cuts for single-scatter nuclear recoils was measured as a function of energy based on a combination of masked WIMP search and neutron calibration data. Most cuts have very little effect on our acceptance of true nuclear recoils, with the ionization-based fiducial volume and phonon-timing cuts imposing the highest costs in signal acceptance (both measured on neutron calibration data). The combined livetime-weighted signal acceptance for

event-specific cuts (i.e. excluding discarded data periods) summed across all Ge detectors included in this analysis is shown in Figure 2. The raw exposure of this analysis is 397.8 kg-days before the cuts shown in Figure 2.

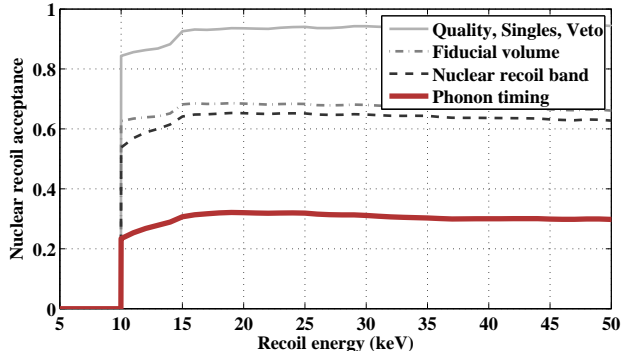


FIG. 2: Nuclear recoil acceptance efficiency as a function of recoil energy, averaged over all detectors included in the present analysis. The four curves represent the estimated total efficiencies at various stages during the analysis, culminating with the efficiency applied to determine the sensitivity limit at the bottom.

After all analysis cuts were finalized and leakage estimation schemes selected, we unmasked the WIMP search signal region on February 4, 2008. No event was observed within the signal region. Figure 3 is a compilation of the low yield events observed in all detectors used in this analysis. It shows the ionization yield distribution versus energy for single-scatter events passing all data selection cuts except the timing cut. The four events shown which pass the timing cuts are outside the nuclear-recoil region.

Using standard assumptions about the galactic halo [5] we derived a limit on the spin-independent WIMP-nucleon cross section using Yellin’s Optimum Interval method [16]. Figure 4 shows this upper limit at 90% C.L. (upper solid curve) as a function of possible WIMP masses, with a minimum at $6.6 \times 10^{-44} \text{ cm}^2$ for a 60 GeV/ c^2 WIMP.

Our previous data from Soudan [8–10] have been re-analyzed [17] yielding a slight improvement in sensitivity over our previous publications (upper curve in Figure 4). A combined limit from the above data sets yields the best overall sensitivity (lower solid curve in Figure 4), giving an upper limit of $4.6 \times 10^{-44} \text{ cm}^2$ at 90% C.L. for a WIMP mass of 60 GeV/ c^2 , a factor of ~ 3 more sensitive than our previously published limit. For comparison, the diagram includes the best previously published limit on the spin-independent WIMP-nucleon cross section from the XENON10 experiment [18] and parameter ranges expected from selected supersymmetric calculations [19, 20].

We also analyzed our data in terms of spin dependent WIMP-nucleon interactions. Under the assumption of spin dependent coupling to neutrons alone and using the

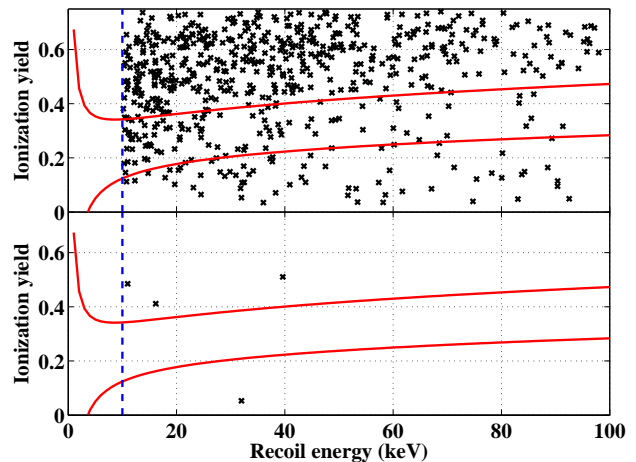


FIG. 3: Top: Ionization yield versus recoil energy in all detectors included in this analysis for events passing all cuts except the ionization yield and surface electron recoil rejection cuts. The signal region between 10 and 100 keV recoil energies was defined using neutron calibration data and is indicated by the curved lines. Bulk electron recoils with yield near unity are above the vertical scale limits. Bottom: Same, but after applying the surface electron recoil rejection cuts. No events are seen within the signal region.

Ge form factor given in [21], we find a minimum upper limit of $2.7 \times 10^{-38} \text{ cm}^2$ ($1.8 \times 10^{-38} \text{ cm}^2$) at 90% C.L. for this data set (combined Soudan data).

CDMS has maintained high discovery potential by limiting expected backgrounds to less than one event in the signal region. These results from our Soudan measurements set the best WIMP sensitivity for spin-independent WIMP-nucleon interactions over a wide range of WIMP masses. Our new limits cut significantly into previously unexplored regions of the central parameter space predicted by supersymmetry excluding some of the favored models.

The CDMS collaboration gratefully acknowledges Patrizia Meunier, Samuel Burke, Daniel Callahan, Pat Castle, Dave Hale, Susanne Kyre, Bruce Lambin and Wayne Johnson for their technical contributions. This work is supported in part by the National Science Foundation (Grant Nos. AST-9978911, PHY-0542066, PHY-0503729, PHY-0503629, PHY-0503641, PHY-0504224 and PHY-0705052), by the Department of Energy under contracts DE-AC03-76SF00098, DE-FG02-91ER40688, DE-FG03-90ER40569, and DE-FG03-91ER40618, by the Swiss National Foundation SNF Grant No 20-118119, and by NSERC Canada via Grant SAPIN 341314-07.

-
- [1] D.N. Spergel *et al.*, (WMAP Collab.), *Astrophys. J. Suppl.* **148**, 175 (2003); M. Tegmark *et al.*, (SDSS Collab.), *Phys. Rev. D* **69**, 103501 (2004).
[2] G. Steigman and M.S. Turner, *Nucl. Phys.* **B253**, 375

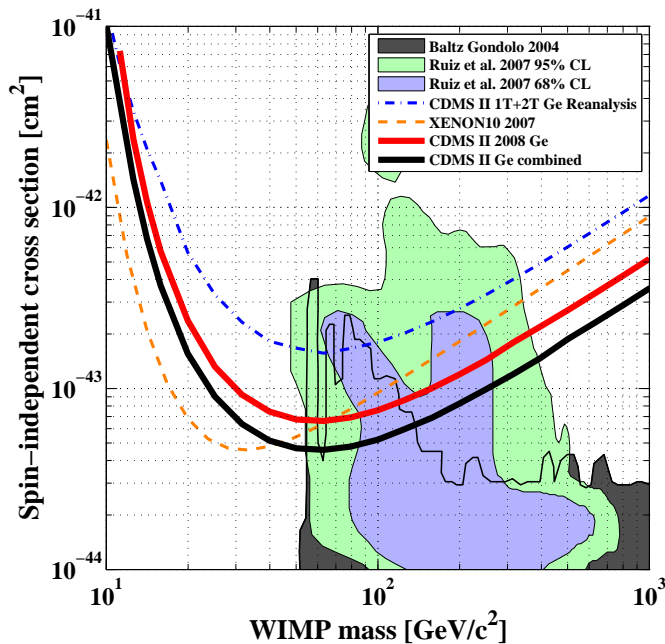


FIG. 4: Spin-independent WIMP-nucleon cross section upper limits (90% C.L.) versus WIMP mass. The upper curve (dash-dot) is the result of a re-analysis [17] of our previously published data. The upper solid line represents the limit derived from our new data set. The combined CDMS limit (lower solid line) reaches the same minimum cross section as that from Xenon10 [18] (dashed), but with more sensitivity at higher masses. Also shown are parameter ranges expected from different supersymmetric models described in [19] (grey) and [20] (95% and 68% confidence levels in green and blue, respectively). Plots courtesy of [22].

(1985).

- [3] B.W. Lee and S. Weinberg, Phys. Rev. Lett. **39**, 165 (1977); S. Weinberg, Phys. Rev. Lett. **48**, 1303 (1982).
- [4] G. Jungman, M. Kamionkowski, and K. Griest, Phys. Rep. **267**, 195 (1996); G. Bertone, D. Hooper, and J. Silk, Phys. Rep. **405**, 279 (2005).
- [5] J.D. Lewin and P.F. Smith, Astropart. Phys. **6**, 87 (1996).
- [6] E.A. Baltz, M. Battaglia, M.E. Peskin and T. Wizansky, Phys. Rev. D **74**, 103521 (2006).
- [7] K.D. Irwin *et al.*, Rev. Sci. Instr. **66**, 5322 (1995); T. Saab *et al.*, AIP Proc. **605**, 497 (2002).
- [8] D.S. Akerib *et al.*, (CDMS Collab.) Phys. Rev. D **72**, 052009 (2005).
- [9] D.S. Akerib *et al.*, (CDMS Collab.) Phys. Rev. Lett. **96**, 011302 (2006).
- [10] D.S. Akerib *et al.*, (CDMS Collab.) Phys. Rev. D **73**, 011102 (2006).
- [11] CDMS Collab., in preparation.
- [12] A. Fassò *et al.*, CERN-2005-10 (2005), INFN/TC.05/11, SLAC-R-773; A. Fassò *et al.*, arXiv:hep-ph/0306167
- [13] J.S. Hendricks *et al.*, LA-UR-07-6632 available from <http://mcnpx.lanl.gov/>
- [14] J. Allison *et al.*, IEEE Trans. Nucl. Sc. **53** (2006) 270; S. Agostinelli *et al.*, Nucl. Instrum. Methods A **506** (2003) 250
- [15] D.S. Leonard *et al.*, (EXO Collab.) arXiv:0709.4524v1 [physics.ins-det].
- [16] S. Yellin, Phys. Rev. D **66**, 032005 (2002).
- [17] CDMS Collab., in preparation; R.W. Ogburn, Ph.D. dissertation. Stanford University (unpublished).
- [18] J. Angle *et al.*, (XENON Collab.) Phys. Rev. Lett. **100**, 021303 (2008)
- [19] E.A. Baltz and P. Gondolo, JHEP 0410 (2004) 052.
- [20] L. Roszkowski *et al.* JHEP 07 (2007) 075.
- [21] J. Engel, Phys. Lett. B **264**, 114 (1991).
- [22] R.J. Gaitskell, V. Mandic and J. Filippini, <http://dmttools.brown.edu>